

CERN-PH-EP-2010-066
2 December 2010

Suppression of charged particle production at large transverse momentum in central Pb–Pb collisions at $\sqrt{s_{NN}} = 2.76$ TeV

ALICE Collaboration*

Abstract

Inclusive transverse momentum spectra of primary charged particles in Pb–Pb collisions at $\sqrt{s_{NN}} = 2.76$ TeV have been measured by the ALICE Collaboration at the LHC. The data are presented for central and peripheral collisions, corresponding to 0–5% and 70–80% of the hadronic Pb–Pb cross section. The measured charged particle spectra in $|\eta| < 0.8$ and $0.3 < p_T < 20$ GeV/c are compared to the expectation in pp collisions at the same $\sqrt{s_{NN}}$, scaled by the number of underlying nucleon–nucleon collisions. The comparison is expressed in terms of the nuclear modification factor R_{AA} . The result indicates only weak medium effects ($R_{AA} \approx 0.7$) in peripheral collisions. In central collisions, R_{AA} reaches a minimum of about 0.14 at $p_T = 6–7$ GeV/c and increases significantly at larger p_T . The measured suppression of high- p_T particles is stronger than that observed at lower collision energies, indicating that a very dense medium is formed in central Pb–Pb collisions at the LHC.

*See Appendix A for the list of collaboration members

High energy heavy-ion collisions enable the study of strongly interacting matter under extreme conditions. At sufficiently high collision energies Quantum-Chromodynamics (QCD) predicts that hot and dense deconfined matter, commonly referred to as the Quark-Gluon Plasma (QGP), is formed. With the advent of a new generation of experiments at the CERN Large Hadron Collider (LHC) [1] a new energy domain is accessible to study the properties of this state.

Previous experiments at the Relativistic Heavy Ion Collider (RHIC) reported that hadron production at high transverse momentum (p_T) in central (head-on) Au–Au collisions at a centre-of-mass energy per nucleon pair $\sqrt{s_{NN}}$ of 200 GeV is suppressed by a factor 4–5 compared to expectations from an independent superposition of nucleon-nucleon (NN) collisions [2, 3, 4, 5]. The dominant production mechanism for high- p_T hadrons is the fragmentation of high- p_T partons that originate in hard scatterings in the early stage of the nuclear collision. The observed suppression at RHIC is generally attributed to energy loss of the partons as they propagate through the hot and dense QCD medium [6, 7, 8, 9, 10].

To quantify nuclear medium effects at high p_T , the so called *nuclear modification factor* R_{AA} is used. R_{AA} is defined as the ratio of the charged particle yield in Pb–Pb to that in pp, scaled by the number of binary nucleon–nucleon collisions $\langle N_{\text{coll}} \rangle$

$$R_{AA}(p_T) = \frac{(1/N_{\text{evt}}^{AA}) d^2N_{\text{ch}}^{AA}/d\eta dp_T}{\langle N_{\text{coll}} \rangle (1/N_{\text{evt}}^{pp}) d^2N_{\text{ch}}^{pp}/d\eta dp_T},$$

where $\eta = -\ln(\tan \theta/2)$ is the pseudo-rapidity and θ is the polar angle between the charged particle direction and the beam axis. The number of binary nucleon–nucleon collisions $\langle N_{\text{coll}} \rangle$ is given by the product of the nuclear overlap function $\langle T_{AA} \rangle$ [11] and the inelastic NN cross section $\sigma_{\text{inel}}^{NN}$. If no nuclear modification is present, R_{AA} is unity at high p_T .

At the larger LHC energy the density of the medium is expected to be higher than at RHIC, leading to a larger energy loss of high p_T partons. On the other hand, the less steeply falling spectrum at the higher energy will lead to a smaller suppression in the p_T spectrum of charged particles, for a given magnitude of partonic energy loss [9, 10]. Both the value of R_{AA} in central collisions as well as its p_T dependence may also in part be influenced by gluon shadowing and saturation effects, which in general decrease with increasing x and Q^2 .

This Letter reports the measurement of the inclusive primary charged particle transverse momentum distributions at mid-rapidity in central and peripheral Pb–Pb collisions at $\sqrt{s_{NN}} = 2.76$ TeV by the ALICE experiment [12]. Primary particles are defined as prompt particles produced in the collision, including decay products, except those from weak decays of strange particles. The data were collected in the first heavy-ion collision period at the LHC. A detailed description of the experiment can be found in [12].

For the present analysis, charged particle tracking utilizes the Inner Tracking System (ITS) and the Time Projection Chamber (TPC) [13], both of which cover the central region in the pseudo-rapidity range $|\eta| < 0.9$. The ITS and TPC detectors are located in the ALICE central barrel and operate in the 0.5 T magnetic field of a large solenoidal magnet. The TPC is a cylindrical drift detector with two readout planes on the endcaps. The active volume covers $85 < r < 247$ cm and $-250 < z < 250$ cm in the radial and longitudinal directions, respectively. A high voltage membrane at $z = 0$ divides the active volume into two halves and provides the electric drift field of 400 V/cm, resulting in a maximum drift time of 94 μs .

The ITS is used for charged particle tracking and trigger purposes. It is composed of six cylindrical layers of high resolution silicon tracking detectors with radial distances to the beam line from 3.9 to 43 cm. The two innermost layers are the Silicon Pixel Detectors (SPD) with a total of 9.8 million pixels, read out by 1200 chips. Each chip provides a fast signal if at least one of its pixels is hit. The signals from the 1200 chips are combined in a programmable logic unit which supplies a trigger signal. The SPD contributes to the minimum-bias trigger, if hits are detected on at least two chips on the outer layer. The SPD is

Table 1: The average numbers of participating nucleons $\langle N_{\text{part}} \rangle$, binary nucleon–nucleon collisions $\langle N_{\text{coll}} \rangle$, and the average nuclear overlap function $\langle T_{AA} \rangle$ for the two centrality bins, expressed in percentages of the hadronic cross section.

Centrality	$\langle N_{\text{part}} \rangle$	$\langle N_{\text{coll}} \rangle$	$\langle T_{AA} \rangle (\text{mb}^{-1})$
0–5%	383 ± 2	1690 ± 131	26.4 ± 0.5
70–80%	15.4 ± 0.4	15.7 ± 0.7	0.25 ± 0.01

followed by two layers of Silicon Drift Detectors (SDD) with 133k readout channels. The two outermost layers are Silicon Strip Detectors (SSD) consisting of double-sided silicon micro-strip sensors, for a total of 2.6 million readout channels.

The two forward scintillator hodoscopes (VZERO-A and VZERO-C) cover the pseudo-rapidity ranges $2.8 < \eta < 5.1$ and $-3.7 < \eta < -1.7$. The sum of the amplitudes of the signals in the VZERO scintillators is used as a measure for the event centrality. The VZERO detectors also provide a fast trigger signal if at least one particle hit was detected.

During the heavy-ion data-taking period, up to 114 bunches, each containing about 7×10^7 ions of ^{208}Pb , were collided at $\sqrt{s_{NN}} = 2.76$ TeV in the ALICE interaction region. The rate of hadronic events was about 100 Hz, corresponding to an estimated luminosity of $1.3 \times 10^{25} \text{ cm}^{-2}\text{s}^{-1}$. The detector readout was triggered by the LHC bunch-crossing signal and a minimum-bias interaction trigger based on trigger signals from VZERO-A, VZERO-C, and SPD. The present analysis combines runs taken with two different minimum-bias conditions. In the first set of runs, two out of the three trigger signals were required, while in the second set a coincidence between VZERO-A and VZERO-C was used. Both trigger conditions have similar efficiency for hadronic interactions, but the latter suppresses a large fraction of electromagnetic reactions.

The following analysis is based on 2.3×10^6 minimum-bias Pb–Pb events, which passed the offline event selection. This selection is based on VZERO timing information and the correlation between TPC tracks and hits in the SPD to reject background events coming from parasitic beam interactions. Additionally, a minimal energy deposit in the Zero Degree Calorimeters (ZDC) is required to further suppress electromagnetic interactions. Only events with reconstructed vertex at $|z_{\text{vtx}}| < 10$ cm were used. The definition of the event centrality is based on the sum of the amplitudes measured in the VZERO detectors as described in [14]. Alternative centrality measures utilize the cluster multiplicity in the outer layer of the SPD or the multiplicity of reconstructed tracks. The correlation between the VZERO amplitude and the uncorrected TPC track multiplicity in $|\eta| < 0.8$ is illustrated in Fig.1. The VZERO amplitude distribution is fitted using a Glauber model [11] to determine percentage intervals of the hadronic cross section, as described in [14]. We used a Glauber model Monte Carlo simulation assuming $\sigma_{\text{inel}}^{NN} = 64$ mb, a Woods-Saxon nuclear density with radius 6.62 ± 0.06 fm and surface diffuseness 0.546 ± 0.010 fm [15]. A minimum inter-nucleon distance of 0.4 ± 0.4 fm is assumed. The Glauber Monte Carlo allows one to relate the event classes to the mean numbers of participating nucleons $\langle N_{\text{part}} \rangle$ and binary collisions $\langle N_{\text{coll}} \rangle$ (see Table 1) by geometrically ordering events according to the impact parameter distribution. The errors include the experimental uncertainties in the parameters used in the Glauber simulation and an uncertainty of ± 5 mb in $\sigma_{\text{inel}}^{NN}$. The TPC multiplicity distributions for the central and peripheral event samples selected for this analysis, corresponding to the 0–5% and 70–80% most central fraction of the hadronic Pb–Pb cross section, are shown in the lower panel of Fig. 1. Charged particle tracks are reconstructed in the ITS and TPC detectors. Track candidates in the TPC are selected in the pseudo-rapidity range $|\eta| < 0.8$. Track quality cuts in the TPC are based on the number of reconstructed space points (at least 70 out of a maximum of 159) and the χ^2 per space point of the momentum fit (lower than 4). The TPC track candidates are projected to the ITS and used for further analysis, if at least two matching

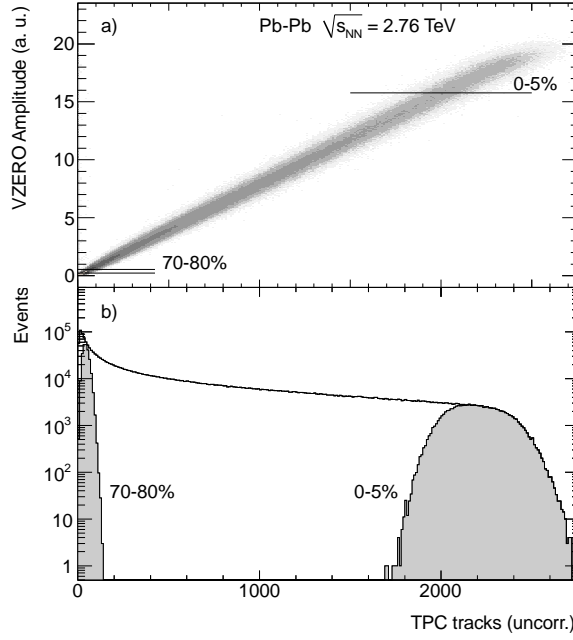


Figure 1: Upper panel: Correlation between VZERO amplitude and the uncorrected track multiplicity in the TPC. Indicated are the cuts for the centrality ranges used in this analysis. Lower panel: Minimum-bias distribution of the TPC track multiplicity. The central (0–5%) and peripheral (70–80%) event subsamples used for this analysis are shown as grey histograms.

hits in the ITS are found, including at least one in the SPD. The average number of associated hits in the ITS is 4.7 for the selected tracks. The event vertex is reconstructed by extrapolating the particle tracks to the interaction region. The event vertex reconstruction is fully efficient in both the peripheral and the central event sample. Tracks are rejected from the final sample if their distance of closest approach to the reconstructed vertex in longitudinal and radial direction, d_z and d_{xy} , satisfies $d_z > 2$ cm or $d_{xy} > 0.018 \text{ cm} + 0.035 \text{ cm} \cdot p_T^{-1.01}$, with p_T in GeV/c.

The efficiency and purity of primary charged particles using these cuts are estimated using a Monte Carlo simulation including HIJING [16] events and a GEANT3 [17] model of the detector response [18]. We used a HIJING tune which reproduces approximately the measured charged particle density in central collisions [14]. In central events, the overall primary charged particle efficiency in $|\eta| < 0.8$ is 60% at $p_T = 0.3$ GeV/c and increases to 65% at $p_T = 0.6$ GeV/c and above. In peripheral events, the efficiency is larger by about 2–3%. The contamination from secondaries is 6% at $p_T = 0.3$ GeV/c and decreases to about 2% at $p_T > 1$ GeV/c, with no significant centrality dependence. This contribution was estimated using the d_{xy} distributions of data and HIJING and is consistent with a first estimate of the strangeness to charged particle ratio from the reconstruction of K_s^0 , Λ and $\bar{\Lambda}$ invariant mass peaks.

The momentum of charged particles is reconstructed from the track curvature measured in the ITS and TPC. The momentum resolution can be parametrized as $(\sigma(p_T)/p_T)^2 = a^2 + (b \cdot p_T)^2$. It is estimated from the track residuals to the momentum fit and verified by cosmic muon events and the width of the invariant mass peaks of Λ , $\bar{\Lambda}$ and K_s^0 . While $a = 0.01$ for both centrality bins, there is a weak centrality dependence of b , i.e. $b = 0.0045$ (GeV/c) $^{-1}$ in peripheral events and $b = 0.0056$ (GeV/c) $^{-1}$ in central events. This is related to a slight decrease for more central events of the average number of space points in the TPC. The modification of the spectra arising from the finite momentum resolution is estimated by Monte Carlo. It results in an overestimate of the yield by up to 8% at $p_T = 20$ GeV/c in central events. This was accounted for by introducing a p_T dependent correction factor to the p_T spectra. From the mass difference between Λ and $\bar{\Lambda}$ and the ratio of positive over negative charged tracks, assuming charge

Table 2: Contributions to the systematic uncertainties on the inclusive spectra. For the p_T dependent errors the ranges are given.

Centrality class	0–5%	70–80%
Centrality selection	1%	7%
Track and event selection cuts	1–4%	1–4%
Particle composition	1–4%	1–4%
Material budget	1–2%	1–2%
Secondary particle rejection	<1%	<1%
Tracking efficiency	2–6%	2–6%
Total systematic uncertainties	5–7%	8–10%

symmetry at high p_T , the upper limit of the systematic uncertainty of the momentum scale is estimated to be $|\Delta(p_T)/p_T| < 0.002$. This has negligible effect on the measured spectra.

Table 2 shows the systematic uncertainties obtained by a comparison of different centrality measures (using the SPD instead of VZERO), and by varying the track and event quality cuts and the Monte Carlo assumptions. In particular, we studied a variation of the most abundant charged particle species (p, π , K) by $\pm 30\%$, the material budget by $\pm 7\%$, and the secondary yield from strangeness decays in the Monte Carlo by $\pm 30\%$. We have used the differences between the standard analysis and one based only on the use of TPC tracks to estimate the uncertainty on the track efficiency corrections, included in the systematic errors. The total systematic uncertainties on the corrected p_T spectra depend on p_T and are 8–10% and 5–7% for the peripheral and central event samples, respectively.

The determination of R_{AA} requires a pp reference at $\sqrt{s} = 2.76$ TeV, where no pp measurement exists. Different approaches are at hand which allow a prediction of the p_T spectrum at a given \sqrt{s} by scaling existing data at different energies. Such approaches assume general scaling properties of perturbative QCD (pQCD) or rely on next-to-leading order (NLO) pQCD calculations. The present analysis follows a data-driven approach with minimal theoretical assumptions where, in order to minimize systematic uncertainties, only measurements by ALICE are considered. In this approach, the pp reference spectrum is obtained by interpolating the differential yields $d^2N_{ch}^{pp}/d\eta dp_T$ of charged particles measured in inelastic pp collisions at $\sqrt{s} = 0.9$ and 7 TeV by ALICE [19, 20]. The interpolation is performed in bins of p_T , based on the assumption that the increase of the yield with \sqrt{s} follows a power law. Above $p_T = 2$ GeV/c, the measured spectra at the two energies are parametrized by a modified Hagedorn function [21] and a power law to reduce bin-by-bin fluctuations. Systematic uncertainties on the pp reference spectrum arise from the experimental errors of the measured spectra at 0.9 and 7 TeV, from the parametrization, and from the interpolation procedure in \sqrt{s} . The combined statistical and systematic data errors result in a 9–10% uncertainty on the pp reference spectrum at $\sqrt{s} = 2.76$ TeV, depending on p_T . The interpolation procedure was verified using PHOJET [22] and PYTHIA [23] (tunes D6T [24] and Perugia0 [25]) at 0.9, 2.76 and 7 TeV. The generated and interpolated spectra at 2.76 TeV agree within the quoted uncertainties. Finally, the scaled pp yield in a given centrality class is obtained by multiplication of the pp reference spectrum with $\langle N_{coll} \rangle$, see Table 1. The uncertainty in $\langle N_{coll} \rangle$ results in an additional p_T -independent scaling uncertainty on the scaled pp reference.

Alternative approaches to derive the pp reference spectrum are investigated to study the sensitivity of R_{AA} to the specific choice of our method. Replacing in the interpolation the p_T spectrum at 0.9 TeV by the one measured in p \bar{p} at $\sqrt{s} = 1.96$ TeV in $|\eta| < 1$ by the CDF collaboration [26] results in a pp reference spectrum which is 5–15% lower than the reference spectrum described above. A different procedure to obtain a pp reference is based on a scaling of the p_T spectra at 0.9 or 7 TeV to 2.76 TeV by the relative \sqrt{s} dependence predicted by NLO pQCD calculations [27] (referred to as “NLO scaling”). Using the

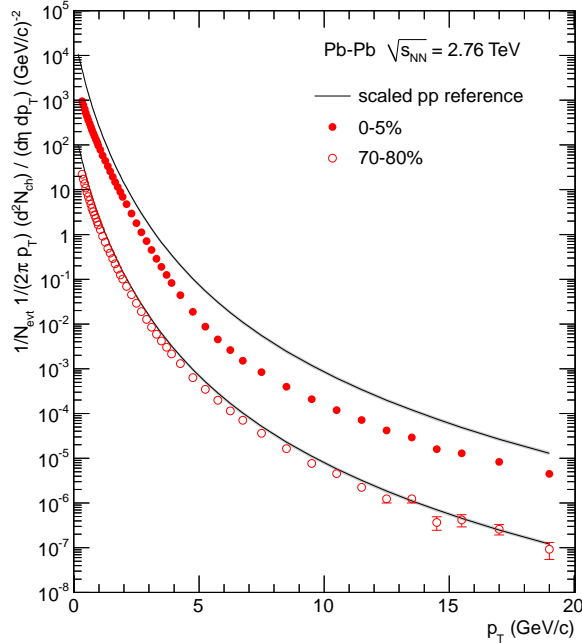


Figure 2: The p_T distributions of primary charged particles at mid-rapidity ($|\eta| < 0.8$) in central (0–5%) and peripheral (70–80%) Pb–Pb collisions at $\sqrt{s_{NN}} = 2.76$ TeV. Error bars are statistical only. The systematic data errors are smaller than the symbols. The scaled pp references are shown as the two curves, the upper for 0–5% centrality and the lower for 70–80%. The systematic uncertainties of the pp reference spectra are contained within the thickness of the line.

7 TeV spectrum as a starting point, good agreement with the reference obtained from interpolation is found. Starting instead from 0.9 TeV results in a spectrum which is 30–50% higher than the interpolation reference. The pp reference spectra derived from the use of the CDF data in the interpolation and from NLO scaling of the 0.9 TeV data are used in the following to illustrate the dependence of R_{AA} at high p_T on the choice of the reference spectrum.

The p_T distributions of primary charged particles in central and peripheral Pb–Pb collisions at 2.76 TeV are shown in Fig. 2, together with the binary-scaled yields from pp collisions. The p_T -dependence is similar for the pp reference and for peripheral Pb–Pb collisions, exhibiting a power law behaviour at $p_T > 3$ GeV/c, which is characteristic of perturbative parton scattering and vacuum fragmentation. In contrast, the spectral shape in central collisions clearly deviates from the scaled pp reference and is closer to an exponential in the p_T range below 5 GeV/c.

Figure 3 shows the nuclear modification factor R_{AA} for central and peripheral Pb–Pb collisions. The nuclear modification factor deviates from one in both samples. At high p_T , where production from hard processes is expected to dominate, there is a marked difference between peripheral and central events. In peripheral collisions, the nuclear modification factor reaches about 0.7 and shows no pronounced p_T dependence for $p_T > 2$ GeV/c. In central collisions, R_{AA} is again significantly different from one, reaching a minimum of $R_{AA} \approx 0.14$ at $p_T = 6$ –7 GeV/c. In the intermediate region there is a strong dependence on p_T with a maximum at $p_T = 2$ GeV/c. This may reflect a variation of the particle composition in heavy-ion collisions with respect to pp, as observed at RHIC [28, 29]. A significant rise of R_{AA} by about a factor of two is observed for $7 < p_T < 20$ GeV/c. Shown as histograms in Fig. 3, for central events only, are the results for R_{AA} at high p_T , using alternative procedures for the computation of the pp reference, as described above. For such scenarios, the overall value for R_{AA} is shifted, but a significant increase of R_{AA} in central collisions for $p_T > 7$ GeV/c persists.

In Fig. 4 the ALICE result in central Pb–Pb collisions at the LHC is compared to measurements of

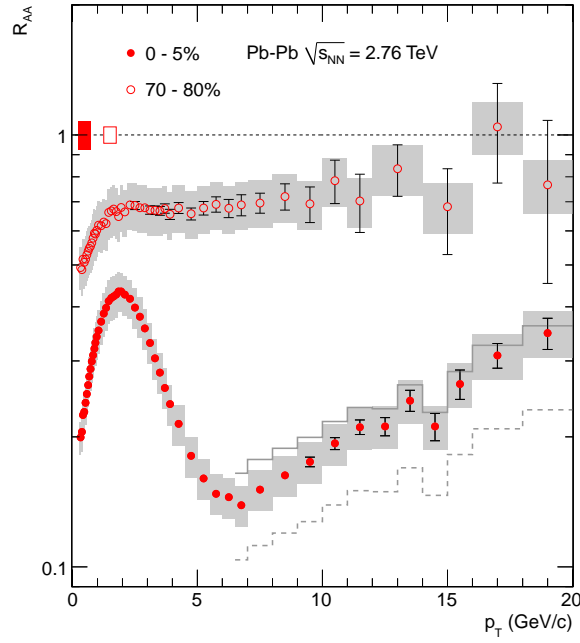


Figure 3: R_{AA} in central (0–5%) and peripheral (70–80%) Pb–Pb collisions at $\sqrt{s_{NN}} = 2.76$ TeV. Error bars indicate the statistical uncertainties. The boxes contain the systematic errors in the data and the p_T dependent systematic errors on the pp reference, added in quadrature. The histograms indicate, for central collisions only, the result for R_{AA} at $p_T > 6.5$ GeV/c using alternative pp references obtained by the use of the $p\bar{p}$ measurement at $\sqrt{s_{NN}} = 1.96$ TeV [26] in the interpolation procedure (solid) and by applying NLO scaling to the pp data at 0.9 TeV (dashed) (see text). The vertical bars around $R_{AA} = 1$ show the p_T independent uncertainty on $\langle N_{coll} \rangle$.

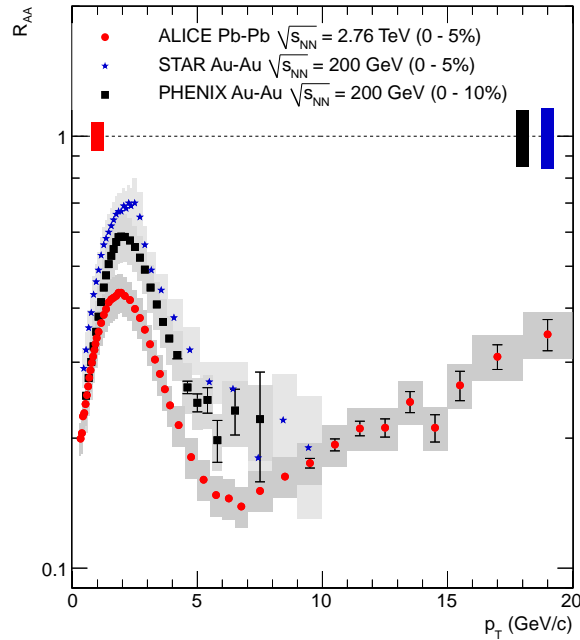


Figure 4: Comparison of R_{AA} in central Pb–Pb collisions at LHC to measurements at $\sqrt{s_{NN}} = 200$ GeV by the PHENIX [30] and STAR [31] experiments at RHIC. The error representation of the ALICE data is as in Fig. 3. The statistical and systematic errors of the PHENIX data are shown as error bars and boxes, respectively. The statistical and systematic errors of the STAR data are combined and shown as boxes. The vertical bars around $R_{AA} = 1$ indicate the p_T independent scaling errors on R_{AA} .

R_{AA} of charged hadrons ($\sqrt{s_{NN}} = 200$ GeV) by the PHENIX and STAR experiments [30, 31] at RHIC. At 1 GeV/c the measured value of R_{AA} is similar to those from RHIC. The position and shape of the maximum at $p_T \sim 2$ GeV/c and the subsequent decrease are similar at RHIC and LHC, contrary to expectations from a recombination model [32]. Despite the much flatter p_T spectrum in pp at the LHC, the nuclear modification factor at $p_T = 6\text{--}7$ GeV/c is smaller than at RHIC. This suggests an enhanced energy loss at LHC and therefore a denser medium. A quantitative determination of the energy loss and medium density will require further investigation of gluon shadowing and saturation in the present energy range and detailed theoretical modeling.

In summary, we have measured the primary charged particle p_T spectra and nuclear modification factors R_{AA} in central (0–5%) and peripheral (70–80%) Pb–Pb collisions at $\sqrt{s_{NN}} = 2.76$ TeV with the ALICE experiment. The nuclear modification factor in peripheral collisions is large and independent of p_T for $p_T > 2$ GeV/c, indicating only weak parton energy loss. For central collisions, the value for R_{AA} is found to be ~ 0.14 at $p_T = 6\text{--}7$ GeV/c, which is smaller than at lower energies, despite the much less steeply falling p_T spectrum at the LHC. Above 7 GeV/c, R_{AA} increases significantly. The observed suppression of high p_T particles provides evidence for strong parton energy loss and large medium density at the LHC.

Acknowledgements

The ALICE collaboration would like to thank all its engineers and technicians for their invaluable contributions to the construction of the experiment and the CERN accelerator teams for the outstanding performance of the LHC complex. The ALICE collaboration acknowledges the following funding agencies for their support in building and running the ALICE detector: Calouste Gulbenkian Foundation from Lisbon and Swiss Fonds Kidagan, Armenia; Conselho Nacional de Desenvolvimento Científico e Tecnológico (CNPq), Financiadora de Estudos e Projetos (FINEP), Fundação de Amparo à Pesquisa do Estado de São Paulo (FAPESP); National Natural Science Foundation of China (NSFC), the Chinese Ministry of Education (CMOE) and the Ministry of Science and Technology of China (MSTC); Ministry of Education and Youth of the Czech Republic; Danish Natural Science Research Council, the Carlsberg Foundation and the Danish National Research Foundation; The European Research Council under the European Community’s Seventh Framework Programme; Helsinki Institute of Physics and the Academy of Finland; French CNRS-IN2P3, the ‘Region Pays de Loire’, ‘Region Alsace’, ‘Region Auvergne’ and CEA, France; German BMBF and the Helmholtz Association; Greek Ministry of Research and Technology; Hungarian OTKA and National Office for Research and Technology (NKTH); Department of Atomic Energy and Department of Science and Technology of the Government of India; Istituto Nazionale di Fisica Nucleare (INFN) of Italy; MEXT Grant-in-Aid for Specially Promoted Research, Japan; Joint Institute for Nuclear Research, Dubna; National Research Foundation of Korea (NRF); CONACYT, DGAPA, México, ALFA-EC and the HELEN Program (High-Energy physics Latin-American–European Network); Stichting voor Fundamenteel Onderzoek der Materie (FOM) and the Nederlandse Organisatie voor Wetenschappelijk Onderzoek (NWO), Netherlands; Research Council of Norway (NFR); Polish Ministry of Science and Higher Education; National Authority for Scientific Research - NASR (Autoritatea Națională pentru Cercetare Științifică - ANCS); Federal Agency of Science of the Ministry of Education and Science of Russian Federation, International Science and Technology Center, Russian Academy of Sciences, Russian Federal Agency of Atomic Energy, Russian Federal Agency for Science and Innovations and CERN-INTAS; Ministry of Education of Slovakia; CIEMAT, EELA, Ministerio de Educación y Ciencia of Spain, Xunta de Galicia (Consellería de Educación), CEADEN, Cubaenergía, Cuba, and IAEA (International Atomic Energy Agency); The Ministry of Science and Technology and the National Research Foundation (NRF), South Africa; Swedish Research Council (VR) and Knut & Alice Wallenberg Foundation (KAW); Ukraine Ministry of Education and Science; United Kingdom Science and Technology Facilities Council (STFC); The United States Department of

Energy, the United States National Science Foundation, the State of Texas, and the State of Ohio.

References

- [1] L. Evans and P. Bryant (editors), JINST **3** (2008) S08001.
- [2] I. Arsene *et al.* [BRAHMS Collaboration], Nucl. Phys. A **757** (2005) 1.
- [3] B.B. Back *et al.* [PHOBOS Collaboration], Nucl. Phys. A **757** (2005) 28.
- [4] J. Adams *et al.* [STAR Collaboration], Nucl. Phys. A **757** (2005) 102.
- [5] K. Adcox *et al.* [PHENIX Collaboration], Nucl. Phys. A **757** (2005) 184.
- [6] E. Wang and X. N. Wang, Phys. Rev. Lett. **89** (2002) 162301.
- [7] R. Baier and D. Schiff, JHEP **0609** (2006) 059.
- [8] S. Wicks, W. Horowitz, M. Djordjevic and M. Gyulassy, Nucl. Phys. A **784** (2007) 426.
- [9] I. Vitev, Phys. Lett. B **639** (2006) 38.
- [10] K. J. Eskola, H. Honkanen, C. A. Salgado and U. A. Wiedemann, Nucl. Phys. A **747** (2005) 511.
- [11] M. Miller, K. Reygers, S. Sanders, and P. Steinberg, Ann. Rev. Nucl. Part. Sci. **57** (2007) 205.
- [12] K. Aamodt *et al.* [ALICE Collaboration], JINST **3** (2008) S08002.
- [13] J. Alme *et al.* [ALICE Collaboration], Nucl. Instrum. Meth. A **622** (2010) 316.
- [14] K. Aamodt *et al.* [ALICE Collaboration], *accepted for publication in Phys. Rev. Lett.*, arXiv:1011.3916 [nucl-ex] and K. Aamodt *et al.*, [ALICE Collaboration] *to be published in Phys. Rev. Lett.*
- [15] H. de Vries, C.W. De Jager and C. de Vries, Atomic Data and Nuclear Tables, **36** (1987) 495.
- [16] X.-N. Wang and M. Gyulassy, Phys. Rev. D **44** (1991) 3501; W.-T. Deng, X.-N. Wang, and R. Xu, (2010), arXiv:1008.1841 [hep-ph].
- [17] R. Brun *et al.*, CERN Program Library Long Write-up, W5013, GEANT Detector Description and Simulation Tool (1994).
- [18] R. Brun *et al.*, [ALICE Collaboration], Nucl. Instrum. Meth. A **502** (2003) 339.
- [19] K. Aamodt *et al.* [ALICE Collaboration], Phys. Lett. B **693** (2010) 53.
- [20] ALICE Collaboration, *to be published*.
- [21] R. Hagedorn, Riv. Nuovo Cim. **6** (1983) 1.
- [22] R. Engel, J. Ranft, S. Roesler, Phys. Rev. D **52** (1995) 1459.
- [23] T. Sjöstrand, S. Mrenna, P. Skands, J. High Energy Phys. **0605** (2006) 026.
- [24] M. Albrow *et al.*, Tevatron-for-LHC Conference Report of the QCD Working Group, Fermilab-Conf-06-359, hep-ph/0610012; T. Sjöstrand and P. Skands, Eur. Phys. J. C **39** (2005) 129.
- [25] P. Skands, Contribution to the 1st International Workshop on Multiple Partonic Interactions at the LHC, Perugia, Italy, Oct. 2008, Fermilab-Conf-09-113-T, arXiv:0905.3418 [hep-ph].
- [26] T. Aaltonen *et al.* [CDF Collaboration], Phys. Rev. D **79** (2009) 112005.
- [27] R. Sassot, P. Zurita, and M. Stratmann, Phys. Rev. D **82** (2010) 074011.
- [28] B. I. Abelev *et al.* [STAR Collaboration], Phys. Rev. Lett. **97** (2006) 152301.
- [29] S. S. Adler *et al.* [PHENIX Collaboration], Phys. Rev. C **69** (2004) 034909.
- [30] S. S. Adler *et al.* [PHENIX Collaboration], Phys. Rev. C **69** (2004) 034910.
- [31] J. Adams *et al.* [STAR Collaboration], Phys. Rev. Lett. **91** (2003) 172302.
- [32] R. J. Fries and B. Muller, Eur. Phys. J. C **34** (2004) S279.

A The ALICE Collaboration

K. Aamodt¹, A. Abrahantes Quintana², D. Adamová³, A.M. Adare⁴, M.M. Aggarwal⁵, G. Aglieri Rinella⁶, A.G. Agocs⁷, S. Aguilar Salazar⁸, Z. Ahammed⁹, N. Ahmad¹⁰, A. Ahmad Masoodi¹⁰, S.U. Ahn^{11.i}, A. Akindinov¹², D. Aleksandrov¹³, B. Alessandro¹⁴, R. Alfaro Molina⁸, A. Alici^{15.ii}, A. Alkin¹⁶, E. Almaráz Aviña⁸, T. Alt¹⁷, V. Altini¹⁸, S. Altinpinar¹⁹, I. Altsybeev²⁰, C. Andrei²¹, A. Andronic¹⁹, V. Anguelov^{22.iii.iv}, C. Anson²³, T. Antičić²⁴, F. Antinori²⁵, P. Antonioli²⁶, L. Aphecetche²⁷, H. Appelshäuser²⁸, N. Arbor²⁹, S. Arcelli¹⁵, A. Arend²⁸, N. Armesto³⁰, R. Arnaldi¹⁴, T. Aronsson⁴, I.C. Arsene¹⁹, A. Asryan²⁰, A. Augustinus⁶, R. Averbeck¹⁹, T.C. Awes³¹, J. Äystö³², M.D. Azmi¹⁰, M. Bach¹⁷, A. Badalá³³, Y.W. Baek^{11.i}, S. Bagnasco¹⁴, R. Bailhache²⁸, R. Bala^{34.v}, R. Baldini Ferroli³⁵, A. Baldisseri³⁶, A. Baldit³⁷, J. Bán³⁸, R. Barbera³⁹, F. Barile¹⁸, G.G. Barnaföldi⁷, L.S. Barnby⁴⁰, V. Barret³⁷, J. Bartke⁴¹, M. Basile¹⁵, N. Bastid³⁷, B. Bathen⁴², G. Batigne²⁷, B. Batyunya⁴³, C. Baumann²⁸, I.G. Bearden⁴⁴, H. Beck²⁸, I. Belikov⁴⁵, F. Bellini¹⁵, R. Bellwied^{46.vi}, E. Belmont-Moreno⁸, S. Beole³⁴, I. Berceanu²¹, A. Bercuci²¹, E. Berdermann¹⁹, Y. Berdnikov⁴⁷, L. Betev⁶, A. Bhasin⁴⁸, A.K. Bhati⁵, L. Bianchi³⁴, N. Bianchi⁴⁹, C. Bianchin²⁵, J. Bielčik⁵⁰, J. Bielčiková³, A. Bilandzic⁵¹, E. Biolcati³⁴, A. Blanc³⁷, F. Blanco⁵², F. Blanco⁵³, D. Blau¹³, C. Blume²⁸, M. Boccioni⁶, N. Bock²³, A. Bogdanov⁵⁴, H. Bøggild⁴⁴, M. Bogolyubsky⁵⁵, L. Boldizsár⁷, M. Bombara⁵⁶, C. Bombonati²⁵, J. Book²⁸, H. Borel³⁶, C. Bortolin^{25.vii}, S. Bose⁵⁷, F. Bossú³⁴, M. Botje⁵¹, S. Böttger²², B. Boyer⁵⁸, P. Braun-Munzinger¹⁹, L. Bravina⁵⁹, M. Bregant^{60.viii}, T. Breitner²², M. Broz⁶¹, R. Brun⁶, E. Bruna⁴, G.E. Bruno¹⁸, D. Budnikov⁶², H. Buesching²⁸, O. Busch⁶³, Z. Buthelezi⁶⁴, D. Caffarri²⁵, X. Cai⁶⁵, H. Caines⁴, E. Calvo Villar⁶⁶, P. Camerini⁶⁰, V. Canoa Roman^{6.ix.x}, G. Cara Romeo²⁶, F. Carena⁶, W. Carena⁶, F. Carminati⁶, A. Casanova Díaz⁴⁹, M. Caselle⁶, J. Castillo Castellanos³⁶, V. Catanescu²¹, C. Cavicchioli⁶, P. Cerello¹⁴, B. Chang³², S. Chapeland⁶, J.L. Charvet³⁶, S. Chattopadhyay⁵⁷, S. Chattopadhyay⁹, M. Cherneny⁶⁷, C. Cheshkov⁶⁸, B. Cheynis⁶⁸, E. Chiavassa¹⁴, V. Chibante Barroso⁶, D.D. Chinellato⁶⁹, P. Chochula⁶, M. Chojnacki⁷⁰, P. Christakoglou⁷⁰, C.H. Christensen⁴⁴, P. Christiansen⁷¹, T. Chujo⁷², C. Cicalo⁷³, L. Cifarelli¹⁵, F. Cindolo²⁶, J. Cleymans⁶⁴, F. Coccetti³⁵, J.-P. Coffin⁴⁵, S. Coli¹⁴, G. Conesa Balbastre^{49.xi}, Z. Conesa del Valle^{27.xii}, P. Constantin⁶³, G. Contin⁶⁰, J.G. Contreras⁷⁴, T.M. Cormier⁴⁶, Y. Corrales Morales³⁴, I. Cortés Maldonado⁷⁵, P. Cortese⁷⁶, M.R. Cosentino⁶⁹, F. Costa⁶, M.E. Cotallo⁵², E. Crescio⁷⁴, P. Crochet³⁷, E. Cuautle⁷⁷, L. Cunqueiro⁴⁹, G. D Erasmo¹⁸, A. Dainese^{78.xiii}, H.H. Dalsgaard⁴⁴, A. Danu⁷⁹, D. Das⁵⁷, I. Das⁵⁷, A. Dash⁸⁰, S. Dash¹⁴, S. De⁹, A. De Azevedo Moregula⁴⁹, G.O.V. de Barros⁸¹, A. De Caro⁸², G. de Cataldo⁸³, J. de Cuveland¹⁷, A. De Falco⁸⁴, D. De Gruttola⁸², N. De Marco¹⁴, S. De Pasquale⁸², R. De Remigis¹⁴, R. de Rooij⁷⁰, H. Delagrange²⁷, Y. Delgado Mercado⁶⁶, G. Dellacasa^{76.xiv}, A. Deloff⁸⁵, V. Demanov⁶², E. Dénes⁷, A. Deppman⁸¹, D. Di Bari¹⁸, C. Di Giglio¹⁸, S. Di Liberto⁸⁶, A. Di Mauro⁶, P. Di Nezza⁴⁹, T. Dietel⁴², R. Divià⁶, Ø. Djuvsland¹, A. Dobrin^{46.xv}, T. Dobrowolski⁸⁵, I. Domínguez⁷⁷, B. Dönigus¹⁹, O. Dordic⁵⁹, O. Driga²⁷, A.K. Dubey⁹, J. Dubuisson⁶, L. Ducroux⁶⁸, P. Dupieux³⁷, A.K. Dutta Majumdar⁵⁷, M.R. Dutta Majumdar⁹, D. Elia⁸³, D. Emschermann⁴², H. Engel²², H.A. Erdal⁸⁷, B. Espagnon⁵⁸, M. Estienne²⁷, S. Esumi⁷², D. Evans⁴⁰, S. Evrard⁶, G. Eyyubova⁵⁹, C.W. Fabjan^{6.xvi}, D. Fabris⁸⁸, J. Faivre²⁹, D. Falchieri¹⁵, A. Fantoni⁴⁹, M. Fasel¹⁹, R. Fearick⁶⁴, A. Fedunov⁴³, D. Fehler¹, V. Fekete⁶¹, D. Felea⁷⁹, G. Feofilov²⁰, A. Fernández Téllez⁷⁵, A. Ferretti³⁴, R. Ferretti^{76.xvii}, M.A.S. Figueredo⁸¹, S. Filchagin⁶², R. Fini⁸³, D. Finogeev⁸⁹, F.M. Fionda¹⁸, E.M. Fiore¹⁸, M. Floris⁶, S. Foertsch⁶⁴, P. Foka¹⁹, S. Fokin¹³, E. Fragiaco⁹⁰, M. Fragkiadakis⁹¹, U. Frankenfeld¹⁹, U. Fuchs⁶, F. Furano⁶, C. Furget²⁹, M. Fusco Girard⁸², J.J. Gaardhøje⁴⁴, S. Gadrat²⁹, M. Gagliardi³⁴, A. Gago⁶⁶, M. Gallio³⁴, P. Ganoti^{91.xviii}, C. Garabatos¹⁹, R. Gemme⁷⁶, J. Gerhard¹⁷, M. Germain²⁷, C. Geuna³⁶, A. Gheata⁶, M. Gheata⁶, B. Ghidini¹⁸, P. Ghosh⁹, M.R. Girard⁹², G. Giraudo¹⁴, P. Giubellino^{34.xix}, E. Gladysz-Dziadus⁴¹, P. Glässel⁶³, R. Gomez⁹³, L.H. González-Trueba⁸, P. González-Zamora⁵², H. González Santos⁷⁵, S. Gorbunov¹⁷, S. Gotovac⁹⁴, V. Grabski⁸, R. Grajcarek⁶³, A. Grelli⁷⁰, A. Grigoras⁶, C. Grigoras⁶, V. Grigoriev⁵⁴, A. Grigoryan⁹⁵, S. Grigoryan⁴³, B. Grinyov¹⁶, N. Grion⁹⁰, P. Gros⁷¹, J.F. Grosse-Oetringhaus⁶, J.-Y. Grossiord⁶⁸, R. Grosso⁸⁸, F. Guber⁸⁹, R. Guernane²⁹, C. Guerra Gutierrez⁶⁶, B. Guerzoni¹⁵, K. Gulbrandsen⁴⁴, T. Gunji⁹⁶, A. Gupta⁴⁸, R. Gupta⁴⁸, H. Gutbrod¹⁹, Ø. Haaland¹, C. Hadjidakis⁵⁸, M. Haiduc⁷⁹, H. Hamagaki⁹⁶, G. Hamar⁷, J.W. Harris⁴, M. Hartig²⁸, D. Hasch⁴⁹, D. Hasegan⁷⁹, D. Hatzifotiadou²⁶, A. Hayrapetyan^{95.xvii}, M. Heide⁴², M. Heinz⁴, H. Helstrup⁸⁷, A. Hergelegiu²¹, C. Hernández¹⁹, G. Herrera Corral⁷⁴, N. Herrmann⁶³, K.F. Hetland⁸⁷, B. Hicks⁴, P.T. Hille⁴, B. Hippolyte⁴⁵, T. Horaguchi⁷², Y. Hori⁹⁶, P. Hristov⁶, I. Hřivnáčová⁵⁸, M. Huang¹, S. Huber¹⁹, T.J. Humanic²³, D.S. Hwang⁹⁷, R. Ichou²⁷, R. Ilkaev⁶², I. Ilkiv⁸⁵, M. Inaba⁷², E. Incani⁸⁴, G.M. Innocenti³⁴, P.G. Innocenti⁶, M. Ippolitov¹³, M. Irfan¹⁰, C. Ivan¹⁹, A. Ivanov²⁰, M. Ivanov¹⁹, V. Ivanov⁴⁷, A. Jachoňkowski⁶, P.M. Jacobs⁹⁸, L. Jancurová⁴³, S. Jangal⁴⁵, R. Janik⁶¹, S.P. Jayarathna^{53.xx}, S. Jena⁹⁹, L. Jirdeň⁶, G.T. Jones⁴⁰, P.G. Jones⁴⁰, P. Jovanović⁴⁰, H. Jung¹¹, W. Jung¹¹, A. Jusko⁴⁰, S. Kalcher¹⁷,

P. Kaliňák³⁸, M. Kalisky⁴², T. Kalliokoski³², A. Kalweit¹⁰⁰, R. Kamermans^{70,xiv}, K. Kanaki¹, E. Kang¹¹, J.H. Kang¹⁰¹, V. Kaplin⁵⁴, O. Karavichev⁸⁹, T. Karavicheva⁸⁹, E. Karpechev⁸⁹, A. Kazantsev¹³, U. Keschull²², R. Keidel¹⁰², M.M. Khan¹⁰, A. Khanzadeev⁴⁷, Y. Kharlov⁵⁵, B. Kileng⁸⁷, D.J. Kim³², D.S. Kim¹¹, D.W. Kim¹¹, H.N. Kim¹¹, J.H. Kim⁹⁷, J.S. Kim¹¹, M. Kim¹¹, M. Kim¹⁰¹, S. Kim⁹⁷, S.H. Kim¹¹, S. Kirsch^{6,xxi}, I. Kisel^{22,iv}, S. Kiselev¹², A. Kisiel⁶, J.L. Klay¹⁰³, J. Klein⁶³, C. Klein-Bösing⁴², M. Kliemant²⁸, A. Klovning¹, A. Kluge⁶, M.L. Knichel¹⁹, K. Koch⁶³, M.K. Köhler¹⁹, R. Kolevatsov⁵⁹, A. Kolojvari²⁰, V. Kondratiev²⁰, N. Kondratyeva⁵⁴, A. Konevskih⁸⁹, E. Kornaś⁴¹, C. Kottachchi Kankanamge Don⁴⁶, R. Kour⁴⁰, M. Kowalski⁴¹, S. Kox²⁹, K. Kozlov¹³, J. Kral³², I. Králik³⁸, F. Kramer²⁸, I. Kraus^{100,xxii}, T. Krawutschke^{63,xxiii}, M. Kretz¹⁷, M. Krivda^{40,xxiv}, D. Krumbhorn⁶³, M. Krus⁵⁰, E. Kryshen⁴⁷, M. Krzewicki⁵¹, Y. Kucheriaev¹³, C. Kuhn⁴⁵, P.G. Kuijter⁵¹, P. Kurashvili⁸⁵, A. Kurepin⁸⁹, A.B. Kurepin⁸⁹, A. Kuryakin⁶², S. Kushpil³, V. Kushpil³, M.J. Kweon⁶³, Y. Kwon¹⁰¹, P. La Rocca³⁹, P. Ladrón de Guevara^{52,xxv}, V. Lafage⁵⁸, C. Lara²², D.T. Larsen¹, C. Lazzeroni⁴⁰, Y. Le Bornec⁵⁸, R. Lea⁶⁰, K.S. Lee¹¹, S.C. Lee¹¹, F. Lefèvre²⁷, J. Lehnert²⁸, L. Leistam⁶, M. Lenhardt²⁷, V. Lenti⁸³, I. León Monzón⁹³, H. León Vargas²⁸, P. Lévai⁷, X. Li¹⁰⁴, R. Lietava⁴⁰, S. Lindal⁵⁹, V. Lindenstruth^{22,iv}, C. Lippmann^{6,xxii}, M.A. Lisa²³, L. Liu¹, V.R. Loggins⁴⁶, V. Loginov⁵⁴, S. Lohn⁶, D. Lohner⁶³, C. Loizides⁹⁸, X. Lopez³⁷, M. López Noriega⁵⁸, E. López Torres², G. Løvholden⁵⁹, X.-G. Lu⁶³, P. Luettig²⁸, M. Lunardon²⁵, G. Luparello³⁴, L. Luquin²⁷, C. Luzzi⁶, K. Ma⁶⁵, R. Ma⁴, D.M. Madagodahettige-Don⁵³, A. Maevskaya⁸⁹, M. Mager⁶, D.P. Mahapatra⁸⁰, A. Maire⁴⁵, M. Malaev⁴⁷, I. Maldonado Cervantes⁷⁷, D. Mal'Kevich¹², P. Malzacher¹⁹, A. Mamonov⁶², L. Manceau³⁷, L. Mangotra⁴⁸, V. Manko¹³, F. Manso³⁷, V. Manzari⁸³, Y. Mao^{65,xxvi}, J. Mareš¹⁰⁵, G.V. Margagliotti⁶⁰, A. Margotti²⁶, A. Marín¹⁹, I. Martashvili¹⁰⁶, P. Martinengo⁶, M.I. Martínez⁷⁵, A. Martínez Davalos⁸, G. Martínez García²⁷, Y. Martynov¹⁶, A. Mas²⁷, S. Masciocchi¹⁹, M. Maserà³⁴, A. Masoni⁷³, L. Massacrier⁶⁸, M. Mastro marco⁸³, A. Mastroserio⁶, Z.L. Matthews⁴⁰, A. Matyja^{41,viii}, D. Mayani⁷⁷, G. Mazza¹⁴, M.A. Mazzoni⁸⁶, F. Meddi¹⁰⁷, A. Menchaca-Rocha⁸, P. Mendez Lorenzo⁶, J. Mercado Pérez⁶³, P. Mereu¹⁴, Y. Miake⁷², J. Midori¹⁰⁸, L. Milano³⁴, J. Milosevic^{59,xxvii}, A. Mischke⁷⁰, D. Miśkowiec^{19,xix}, C. Mitu⁷⁹, J. Mlynarz⁴⁶, B. Mohanty⁹, L. Molnar⁶, L. Montaño Zetina⁷⁴, M. Monteno¹⁴, E. Montes⁵², M. Morando²⁵, D.A. Moreira De Godoy⁸¹, S. Moretto²⁵, A. Morsch⁶, V. Muccifora⁴⁹, E. Mudnic⁹⁴, H. Müller⁶, S. Muhuri⁹, M.G. Munhoz⁸¹, J. Munoz⁷⁵, L. Musa⁶, A. Musso¹⁴, B.K. Nandi⁹⁹, R. Nania²⁶, E. Nappi⁸³, C. Nattrass¹⁰⁶, F. Navach¹⁸, S. Navin⁴⁰, T.K. Nayak⁹, S. Nazarenko⁶², G. Nazarov⁶², A. Nedosekin¹², F. Nendaz⁶⁸, J. Newby¹⁰⁹, M. Nicassio¹⁸, B.S. Nielsen⁴⁴, S. Nikolaev¹³, V. Nikolic²⁴, S. Nikulin¹³, V. Nikulin⁴⁷, B.S. Nilsen⁶⁷, M.S. Nilsson⁵⁹, F. Noferini²⁶, G. Nooren⁷⁰, N. Novitzky³², A. Nyanin¹³, A. Nyatha⁹⁹, C. Nygaard⁴⁴, J. Nystrand¹, H. Obayashi¹⁰⁸, A. Ochirov²⁰, H. Oeschler¹⁰⁰, S.K. Oh¹¹, J. Oleniacz⁹², C. Oppedisano¹⁴, A. Ortiz Velasquez⁷⁷, G. Ortona³⁴, A. Oskarsson⁷¹, P. Ostrowski⁹², I. Otterlund⁷¹, J. Otwinowski¹⁹, G. Øvrebek¹, K. Oyama⁶³, K. Ozawa⁹⁶, Y. Pachmayer⁶³, M. Pachr⁵⁰, F. Padilla³⁴, P. Pagano⁸², G. Paic⁷⁷, F. Painke¹⁷, C. Pajares³⁰, S. Pal³⁶, S.K. Pal⁹, A. Palaha⁴⁰, A. Palmeri³³, G.S. Pappalardo³³, W.J. Park¹⁹, V. Paticchio⁸³, A. Pavlinov⁴⁶, T. Pawlak⁹², T. Peitzmann⁷⁰, D. Peresunko¹³, C.E. Pérez Lara⁵¹, D. Perini⁶, D. Perrino¹⁸, W. Peryt⁹², A. Pesci²⁶, V. Peskov⁶, Y. Pestov¹¹⁰, A.J. Peters⁶, V. Petráček⁵⁰, M. Petris²¹, P. Petrov⁴⁰, M. Petrovici²¹, C. Petta³⁹, S. Piano⁹⁰, A. Piccotti¹⁴, M. Pikna⁶¹, P. Pillot²⁷, O. Pinazza⁶, L. Pinsky⁵³, N. Pitz²⁸, F. Piuz⁶, D.B. Piyarathna^{46,xxviii}, R. Platt⁴⁰, M. Płoskoń⁹⁸, J. Pluta⁹², T. Pocheptsov^{43,xxix}, S. Pochybova⁷, P.L.M. Podesta-Lerma⁹³, M.G. Poghosyan³⁴, K. Polák¹⁰⁵, B. Polichtchouk⁵⁵, A. Pop²¹, V. Pospíšil⁵⁰, B. Potukuchi⁴⁸, S.K. Prasad^{46,xxx}, R. Preghenella³⁵, F. Prino¹⁴, C.A. Pruneau⁴⁶, I. Pshenichnov⁸⁹, G. Puudu⁸⁴, A. Pulvirenti³⁹, V. Punin⁶², M. Putiš⁵⁶, J. Putschke⁴, E. Quercigh⁶, H. Qvigstad⁵⁹, A. Rachevski⁹⁰, A. Rademakers⁶, O. Rademakers⁶, S. Radomski⁶³, T.S. Rähä³², J. Rak³², A. Rakotozafindrabe³⁶, L. Ramello⁷⁶, A. Ramírez Reyes⁷⁴, M. Rammler⁴², R. Raniwala¹¹¹, S. Raniwala¹¹¹, S.S. Räsänen³², K.F. Read¹⁰⁶, J.S. Real²⁹, K. Redlich⁸⁵, R. Renfordt²⁸, A.R. Reolon⁴⁹, A. Reshetin⁸⁹, F. Rettig¹⁷, J.-P. Revol⁶, K. Reygers⁶³, H. Ricard¹⁰⁰, L. Riccati¹⁴, R.A. Ricci⁷⁸, M. Richter^{1,xxxi}, P. Riedler⁶, W. Riegler⁶, F. Riggi³⁹, A. Rivetti¹⁴, M. Rodríguez Cahuantzi⁷⁵, D. Rohr¹⁷, D. Röhrich¹, R. Romita¹⁹, F. Ronchetti⁴⁹, P. Rosinský⁶, P. Rosnet³⁷, S. Rossegger⁶, A. Rossi²⁵, F. Roukoutakis⁹¹, S. Rousseau⁵⁸, C. Roy^{27,xii}, P. Roy⁵⁷, A.J. Rubio Montero⁵², R. Rui⁶⁰, I. Rusanov⁶, E. Ryabinkin¹³, A. Rybicki⁴¹, S. Sadovsky⁵⁵, K. Šafařík⁶, R. Sahoo²⁵, P.K. Sahu⁸⁰, P. Saiz⁶, S. Sakai⁹⁸, D. Sakata⁷², C.A. Salgado³⁰, T. Samanta⁹, S. Sambyal⁴⁸, V. Samsonov⁴⁷, L. Šándor³⁸, A. Sandoval⁸, M. Sano⁷², S. Sano⁹⁶, R. Santo⁴², R. Santoro⁸³, J. Sarkamo³², P. Saturnini³⁷, E. Scapparone²⁶, F. Scarlassara²⁵, R.P. Scharenberg¹¹², C. Schiaua²¹, R. Schicker⁶³, C. Schmidt¹⁹, H.R. Schmidt¹⁹, S. Schreiner⁶, S. Schuchmann²⁸, J. Schukraft⁶, Y. Schutz^{27,xvii}, K. Schwarz¹⁹, K. Schweda⁶³, G. Scioli¹⁵, E. Scomparin¹⁴, P.A. Scott⁴⁰, R. Scott¹⁰⁶, G. Segato²⁵, S. Senyukov⁷⁶, J. Seo¹¹, S. Serici⁸⁴, E. Serradilla⁵², A. Sevcenco⁷⁹, G. Shabratova⁴³, R. Shahoyan⁶, N. Sharma⁵, S. Sharma⁴⁸, K. Shigaki¹⁰⁸, M. Shimomura⁷², K. Shtejer², Y. Sibiriak¹³, M. Siciliano³⁴, E. Sicking⁶, T. Siemiarczuk⁸⁵,

A. Silenzi¹⁵, D. Silvermyr³¹, G. Simonetti^{6,xxxiii}, R. Singaraju⁹, R. Singh⁴⁸, B.C. Sinha⁹, T. Sinha⁵⁷, B. Sitar⁶¹, M. Sitta⁷⁶, T.B. Skaali⁵⁹, K. Skjerdal¹, R. Smakal⁵⁰, N. Smirnov⁴, R. Snellings^{51,xxxiii}, C. Søgaard⁴⁴, A. Soloviev⁵⁵, R. Soltz¹⁰⁹, H. Son⁹⁷, M. Song¹⁰¹, C. Soos⁶, F. Soramel²⁵, M. Spyropoulou-Stassinaki⁹¹, B.K. Srivastava¹¹², J. Stachel⁶³, I. Stan⁷⁹, G. Stefanek⁸⁵, G. Stefanini⁶, T. Steinbeck^{22,iv}, E. Stenlund⁷¹, G. Steyn⁶⁴, D. Stocco²⁷, R. Stock²⁸, M. Stolpovskiy⁵⁵, P. Strmen⁶¹, A.A.P. Suaide⁸¹, M.A. Subieta Vásquez³⁴, T. Sugitate¹⁰⁸, C. Suire⁵⁸, M. Šumbera³, T. Susa²⁴, D. Swoboda⁶, T.J.M. Symons⁹⁸, A. Szanto de Toledo⁸¹, I. Szarka⁶¹, A. Szostak¹, C. Tagridis⁹¹, J. Takahashi⁶⁹, J.D. Tapia Takaki⁵⁸, A. Tauro⁶, M. Tavlet⁶, G. Tejeda Muñoz⁷⁵, A. Telesca⁶, C. Terrevoli¹⁸, J. Thäder¹⁹, D. Thomas⁷⁰, J.H. Thomas¹⁹, R. Tieulent⁶⁸, A.R. Timmins^{46,vi}, D. Tlusty⁵⁰, A. Toia⁶, H. Torii¹⁰⁸, L. Toscano⁶, F. Tosello¹⁴, T. Traczyk⁹², D. Truesdale²³, W.H. Trzaska³², A. Tumkin⁶², R. Turrisi⁸⁸, A.J. Turvey⁶⁷, T.S. Tveter⁵⁹, J. Ulery²⁸, K. Ullaland¹, A. Uras⁸⁴, J. Urbán⁵⁶, G.M. Urciuoli⁸⁶, G.L. Usai⁸⁴, A. Vacchi⁹⁰, M. Vala^{43,xxiv}, L. Valencia Palomo⁵⁸, S. Vallero⁶³, N. van der Kolk⁵¹, M. van Leeuwen⁷⁰, P. Vande Vyvre⁶, L. Vannucci⁷⁸, A. Vargas⁷⁵, R. Varma⁹⁹, M. Vasileiou⁹¹, A. Vasiliev¹³, V. Vechernin²⁰, M. Venaruzzo⁶⁰, E. Vercellin³⁴, S. Vergara⁷⁵, R. Vernet¹¹³, M. Verweij⁷⁰, L. Vickovic⁹⁴, G. Viesti²⁵, O. Vikhlyantsev⁶², Z. Vilakazi⁶⁴, O. Villalobos Baillie⁴⁰, A. Vinogradov¹³, L. Vinogradov²⁰, Y. Vinogradov⁶², T. Virgili⁸², Y.P. Viyogi⁹, A. Vodopyanov⁴³, K. Voloshin¹², S. Voloshin⁴⁶, G. Volpe¹⁸, B. von Haller⁶, D. Vranic¹⁹, J. Vrláková⁵⁶, B. Vulpescu³⁷, B. Wagner¹, V. Wagner⁵⁰, R. Wan^{45,xxxiv}, D. Wang⁶⁵, Y. Wang⁶³, Y. Wang⁶⁵, K. Watanabe⁷², J.P. Wessels⁴², U. Westerhoff⁴², J. Wiechula⁶³, J. Wikne⁵⁹, M. Wilde⁴², A. Wilk⁴², G. Wilk⁸⁵, M.C.S. Williams²⁶, B. Windelband⁶³, H. Yang³⁶, S. Yasnopolskiy¹³, J. Yi¹¹⁴, Z. Yin⁶⁵, H. Yokoyama⁷², I.-K. Yoo¹¹⁴, X. Yuan⁶⁵, I. Yushmanov¹³, E. Zabrodin⁵⁹, C. Zampolli⁶, S. Zaporozhets⁴³, A. Zarochentsev²⁰, P. Závada¹⁰⁵, H. Zbroszczyk⁹², P. Zelnicek²², A. Zenin⁵⁵, I. Zgura⁷⁹, M. Zhalov⁴⁷, X. Zhang^{65,i}, D. Zhou⁶⁵, A. Zichichi^{15,xxxv}, G. Zinovjev¹⁶, Y. Zoccarato⁶⁸, M. Zynovyev¹⁶

Affiliation notes

- ⁱ Also at Laboratoire de Physique Corpusculaire (LPC), Clermont Université, Université Blaise Pascal, CNRS-IN2P3, Clermont-Ferrand, France
- ⁱⁱ Now at Centro Fermi – Centro Studi e Ricerche e Museo Storico della Fisica “Enrico Fermi”, Rome, Italy
- ⁱⁱⁱ Now at Physikalisches Institut, Ruprecht-Karls-Universität Heidelberg, Heidelberg, Germany
- ^{iv} Now at Frankfurt Institute for Advanced Studies, Johann Wolfgang Goethe-Universität Frankfurt, Frankfurt, Germany
- ^v Now at Sezione INFN, Turin, Italy
- ^{vi} Now at University of Houston, Houston, Texas, United States
- ^{vii} Also at Dipartimento di Fisica dell’Università, Udine, Italy
- ^{viii} Now at SUBATECH, Ecole des Mines de Nantes, Université de Nantes, CNRS-IN2P3, Nantes, France
- ^{ix} Now at Centro de Investigación y de Estudios Avanzados (CINVESTAV), Mexico City and Mérida, Mexico
- ^x Now at Benemérita Universidad Autónoma de Puebla, Puebla, Mexico
- ^{xi} Now at Laboratoire de Physique Subatomique et de Cosmologie (LPSC), Université Joseph Fourier, CNRS-IN2P3, Institut Polytechnique de Grenoble, Grenoble, France
- ^{xii} Now at Institut Pluridisciplinaire Hubert Curien (IPHC), Université de Strasbourg, CNRS-IN2P3, Strasbourg, France
- ^{xiii} Now at Sezione INFN, Padova, Italy
- ^{xiv} Deceased
- ^{xv} Also at Division of Experimental High Energy Physics, University of Lund, Lund, Sweden
- ^{xvi} Also at University of Technology and Austrian Academy of Sciences, Vienna, Austria
- ^{xvii} Also at European Organization for Nuclear Research (CERN), Geneva, Switzerland
- ^{xviii} Now at Oak Ridge National Laboratory, Oak Ridge, Tennessee, United States
- ^{xix} Now at European Organization for Nuclear Research (CERN), Geneva, Switzerland
- ^{xx} Also at Wayne State University, Detroit, Michigan, United States
- ^{xxi} Also at Frankfurt Institute for Advanced Studies, Johann Wolfgang Goethe-Universität Frankfurt, Frankfurt, Germany
- ^{xxii} Now at Research Division and ExtreMe Matter Institute EMMI, GSI Helmholtzzentrum für Schwerionenforschung, Darmstadt, Germany
- ^{xxiii} Also at Fachhochschule Köln, Köln, Germany
- ^{xxiv} Also at Institute of Experimental Physics, Slovak Academy of Sciences, Košice, Slovakia
- ^{xxv} Now at Instituto de Ciencias Nucleares, Universidad Nacional Autónoma de México, Mexico City, Mexico

- xxvi Also at Laboratoire de Physique Subatomique et de Cosmologie (LPSC), Université Joseph Fourier, CNRS-IN2P3, Institut Polytechnique de Grenoble, Grenoble, France
- xxvii Also at "Vinča" Institute of Nuclear Sciences, Belgrade, Serbia
- xxviii Also at University of Houston, Houston, Texas, United States
- xxix Also at Department of Physics, University of Oslo, Oslo, Norway
- xxx Also at Variable Energy Cyclotron Centre, Kolkata, India
- xxxi Now at Department of Physics, University of Oslo, Oslo, Norway
- xxxii Also at Dipartimento Interateneo di Fisica 'M. Merlin' and Sezione INFN, Bari, Italy
- xxxiii Now at Nikhef, National Institute for Subatomic Physics and Institute for Subatomic Physics of Utrecht University, Utrecht, Netherlands
- xxxiv Also at Hua-Zhong Normal University, Wuhan, China
- xxxv Also at Centro Fermi – Centro Studi e Ricerche e Museo Storico della Fisica "Enrico Fermi", Rome, Italy

Collaboration Institutes

- 1 Department of Physics and Technology, University of Bergen, Bergen, Norway
- 2 Centro de Aplicaciones Tecnológicas y Desarrollo Nuclear (CEADEN), Havana, Cuba
- 3 Nuclear Physics Institute, Academy of Sciences of the Czech Republic, Řež u Prahy, Czech Republic
- 4 Yale University, New Haven, Connecticut, United States
- 5 Physics Department, Panjab University, Chandigarh, India
- 6 European Organization for Nuclear Research (CERN), Geneva, Switzerland
- 7 KFKI Research Institute for Particle and Nuclear Physics, Hungarian Academy of Sciences, Budapest, Hungary
- 8 Instituto de Física, Universidad Nacional Autónoma de México, Mexico City, Mexico
- 9 Variable Energy Cyclotron Centre, Kolkata, India
- 10 Department of Physics Aligarh Muslim University, Aligarh, India
- 11 Gangneung-Wonju National University, Gangneung, South Korea
- 12 Institute for Theoretical and Experimental Physics, Moscow, Russia
- 13 Russian Research Centre Kurchatov Institute, Moscow, Russia
- 14 Sezione INFN, Turin, Italy
- 15 Dipartimento di Fisica dell'Università and Sezione INFN, Bologna, Italy
- 16 Bogolyubov Institute for Theoretical Physics, Kiev, Ukraine
- 17 Frankfurt Institute for Advanced Studies, Johann Wolfgang Goethe-Universität Frankfurt, Frankfurt, Germany
- 18 Dipartimento Interateneo di Fisica 'M. Merlin' and Sezione INFN, Bari, Italy
- 19 Research Division and ExtreMe Matter Institute EMMI, GSI Helmholtzzentrum für Schwerionenforschung, Darmstadt, Germany
- 20 V. Fock Institute for Physics, St. Petersburg State University, St. Petersburg, Russia
- 21 National Institute for Physics and Nuclear Engineering, Bucharest, Romania
- 22 Kirchhoff-Institut für Physik, Ruprecht-Karls-Universität Heidelberg, Heidelberg, Germany
- 23 Department of Physics, Ohio State University, Columbus, Ohio, United States
- 24 Rudjer Bošković Institute, Zagreb, Croatia
- 25 Dipartimento di Fisica dell'Università and Sezione INFN, Padova, Italy
- 26 Sezione INFN, Bologna, Italy
- 27 SUBATECH, Ecole des Mines de Nantes, Université de Nantes, CNRS-IN2P3, Nantes, France
- 28 Institut für Kernphysik, Johann Wolfgang Goethe-Universität Frankfurt, Frankfurt, Germany
- 29 Laboratoire de Physique Subatomique et de Cosmologie (LPSC), Université Joseph Fourier, CNRS-IN2P3, Institut Polytechnique de Grenoble, Grenoble, France
- 30 Departamento de Física de Partículas and IGFAE, Universidad de Santiago de Compostela, Santiago de Compostela, Spain
- 31 Oak Ridge National Laboratory, Oak Ridge, Tennessee, United States
- 32 Helsinki Institute of Physics (HIP) and University of Jyväskylä, Jyväskylä, Finland
- 33 Sezione INFN, Catania, Italy
- 34 Dipartimento di Fisica Sperimentale dell'Università and Sezione INFN, Turin, Italy
- 35 Centro Fermi – Centro Studi e Ricerche e Museo Storico della Fisica "Enrico Fermi", Rome, Italy
- 36 Commissariat à l'Énergie Atomique, IRFU, Saclay, France

- 37 Laboratoire de Physique Corpusculaire (LPC), Clermont Université, Université Blaise Pascal, CNRS-IN2P3, Clermont-Ferrand, France
- 38 Institute of Experimental Physics, Slovak Academy of Sciences, Košice, Slovakia
- 39 Dipartimento di Fisica e Astronomia dell'Università and Sezione INFN, Catania, Italy
- 40 School of Physics and Astronomy, University of Birmingham, Birmingham, United Kingdom
- 41 The Henryk Niewodniczanski Institute of Nuclear Physics, Polish Academy of Sciences, Cracow, Poland
- 42 Institut für Kernphysik, Westfälische Wilhelms-Universität Münster, Münster, Germany
- 43 Joint Institute for Nuclear Research (JINR), Dubna, Russia
- 44 Niels Bohr Institute, University of Copenhagen, Copenhagen, Denmark
- 45 Institut Pluridisciplinaire Hubert Curien (IPHC), Université de Strasbourg, CNRS-IN2P3, Strasbourg, France
- 46 Wayne State University, Detroit, Michigan, United States
- 47 Petersburg Nuclear Physics Institute, Gatchina, Russia
- 48 Physics Department, University of Jammu, Jammu, India
- 49 Laboratori Nazionali di Frascati, INFN, Frascati, Italy
- 50 Faculty of Nuclear Sciences and Physical Engineering, Czech Technical University in Prague, Prague, Czech Republic
- 51 Nikhef, National Institute for Subatomic Physics, Amsterdam, Netherlands
- 52 Centro de Investigaciones Energéticas Medioambientales y Tecnológicas (CIEMAT), Madrid, Spain
- 53 University of Houston, Houston, Texas, United States
- 54 Moscow Engineering Physics Institute, Moscow, Russia
- 55 Institute for High Energy Physics, Protvino, Russia
- 56 Faculty of Science, P.J. Šafárik University, Košice, Slovakia
- 57 Saha Institute of Nuclear Physics, Kolkata, India
- 58 Institut de Physique Nucléaire d'Orsay (IPNO), Université Paris-Sud, CNRS-IN2P3, Orsay, France
- 59 Department of Physics, University of Oslo, Oslo, Norway
- 60 Dipartimento di Fisica dell'Università and Sezione INFN, Trieste, Italy
- 61 Faculty of Mathematics, Physics and Informatics, Comenius University, Bratislava, Slovakia
- 62 Russian Federal Nuclear Center (VNIIEF), Sarov, Russia
- 63 Physikalisches Institut, Ruprecht-Karls-Universität Heidelberg, Heidelberg, Germany
- 64 Physics Department, University of Cape Town, iThemba Laboratories, Cape Town, South Africa
- 65 Hua-Zhong Normal University, Wuhan, China
- 66 Sección Física, Departamento de Ciencias, Pontificia Universidad Católica del Perú, Lima, Peru
- 67 Physics Department, Creighton University, Omaha, Nebraska, United States
- 68 Université de Lyon, Université Lyon 1, CNRS/IN2P3, IPN-Lyon, Villeurbanne, France
- 69 Universidade Estadual de Campinas (UNICAMP), Campinas, Brazil
- 70 Nikhef, National Institute for Subatomic Physics and Institute for Subatomic Physics of Utrecht University, Utrecht, Netherlands
- 71 Division of Experimental High Energy Physics, University of Lund, Lund, Sweden
- 72 University of Tsukuba, Tsukuba, Japan
- 73 Sezione INFN, Cagliari, Italy
- 74 Centro de Investigación y de Estudios Avanzados (CINVESTAV), Mexico City and Mérida, Mexico
- 75 Benemérita Universidad Autónoma de Puebla, Puebla, Mexico
- 76 Dipartimento di Scienze e Tecnologie Avanzate dell'Università del Piemonte Orientale and Gruppo Collegato INFN, Alessandria, Italy
- 77 Instituto de Ciencias Nucleares, Universidad Nacional Autónoma de México, Mexico City, Mexico
- 78 Laboratori Nazionali di Legnaro, INFN, Legnaro, Italy
- 79 Institute of Space Sciences (ISS), Bucharest, Romania
- 80 Institute of Physics, Bhubaneswar, India
- 81 Universidade de São Paulo (USP), São Paulo, Brazil
- 82 Dipartimento di Fisica 'E.R. Caianiello' dell'Università and Gruppo Collegato INFN, Salerno, Italy
- 83 Sezione INFN, Bari, Italy
- 84 Dipartimento di Fisica dell'Università and Sezione INFN, Cagliari, Italy
- 85 Soltan Institute for Nuclear Studies, Warsaw, Poland
- 86 Sezione INFN, Rome, Italy
- 87 Faculty of Engineering, Bergen University College, Bergen, Norway

- 88 Sezione INFN, Padova, Italy
- 89 Institute for Nuclear Research, Academy of Sciences, Moscow, Russia
- 90 Sezione INFN, Trieste, Italy
- 91 Physics Department, University of Athens, Athens, Greece
- 92 Warsaw University of Technology, Warsaw, Poland
- 93 Universidad Autónoma de Sinaloa, Culiacán, Mexico
- 94 Technical University of Split FESB, Split, Croatia
- 95 Yerevan Physics Institute, Yerevan, Armenia
- 96 University of Tokyo, Tokyo, Japan
- 97 Department of Physics, Sejong University, Seoul, South Korea
- 98 Lawrence Berkeley National Laboratory, Berkeley, California, United States
- 99 Indian Institute of Technology, Mumbai, India
- 100 Institut für Kernphysik, Technische Universität Darmstadt, Darmstadt, Germany
- 101 Yonsei University, Seoul, South Korea
- 102 Zentrum für Technologietransfer und Telekommunikation (ZTT), Fachhochschule Worms, Worms, Germany
- 103 California Polytechnic State University, San Luis Obispo, California, United States
- 104 China Institute of Atomic Energy, Beijing, China
- 105 Institute of Physics, Academy of Sciences of the Czech Republic, Prague, Czech Republic
- 106 University of Tennessee, Knoxville, Tennessee, United States
- 107 Dipartimento di Fisica dell'Università 'La Sapienza' and Sezione INFN, Rome, Italy
- 108 Hiroshima University, Hiroshima, Japan
- 109 Lawrence Livermore National Laboratory, Livermore, California, United States
- 110 Budker Institute for Nuclear Physics, Novosibirsk, Russia
- 111 Physics Department, University of Rajasthan, Jaipur, India
- 112 Purdue University, West Lafayette, Indiana, United States
- 113 Centre de Calcul de l'IN2P3, Villeurbanne, France
- 114 Pusan National University, Pusan, South Korea